



UNIVERSITY OF LEEDS

This is a repository copy of *Substantial Increases in Eastern Amazon and Cerrado Biomass Burning-Sourced Tropospheric Ozone*.

White Rose Research Online URL for this paper:

<http://eprints.whiterose.ac.uk/157863/>

Version: Supplemental Material

---

**Article:**

Pope, RJ orcid.org/0000-0002-3587-837X, Arnold, SR orcid.org/0000-0002-4881-5685, Chipperfield, MP orcid.org/0000-0002-6803-4149 et al. (11 more authors) (2020) Substantial Increases in Eastern Amazon and Cerrado Biomass Burning-Sourced Tropospheric Ozone. *Geophysical Research Letters*, 47 (3). e2019GL084143. ISSN 0094-8276

<https://doi.org/10.1029/2019GL084143>

---

© 2019. American Geophysical Union. All Rights Reserved. This is an author produced version of a paper published in *Earth and Planetary Science Letters*. Uploaded in accordance with the publisher's self-archiving policy.

**Reuse**

Items deposited in White Rose Research Online are protected by copyright, with all rights reserved unless indicated otherwise. They may be downloaded and/or printed for private study, or other acts as permitted by national copyright laws. The publisher or other rights holders may allow further reproduction and re-use of the full text version. This is indicated by the licence information on the White Rose Research Online record for the item.

**Takedown**

If you consider content in White Rose Research Online to be in breach of UK law, please notify us by emailing [eprints@whiterose.ac.uk](mailto:eprints@whiterose.ac.uk) including the URL of the record and the reason for the withdrawal request.

# Supplementary Material for “Substantial increases in Eastern Amazon and Cerrado biomass burning-sourced ozone: Impacts on regional air quality”

3 Pope R.J. et al., (Submitted to *Geophysical Research Letters*)

4

## 5 Supplementary Material (SM 1): Satellite Data

## 6 Anomalous *Fire Activity Years*

7 Precipitation data from the Tropical Rainfall Measuring Mission (TRMM) satellite, has suggested that  
8 2005, 2007, 2010 and 2015 can be classed as extreme drought/anomalous fire (ED-AF) years where  
9 fire activity is enhanced across the western Amazon (Reddington et al., 2015; Aragão et al., 2014).

10 We undertook a similar approach to identify ED-AF years in the eastern Amazon (see defined region  
11 in **Figure SM1**: 40–60°W, 0–20°S), but did not find such a significant or distinct signal in this region.

12 The correlation between precipitation and fire activity was also weaker in our study area. Therefore,  
13 as fire activity predominantly controls regional pollution, we used the GFED and GFAS datasets to  
14 identify ED-AF years. **Figure SM1** shows the ASO standardised anomalies for both fire products. ED-  
15 AF years were identified when the standardised anomalies of either product was greater than 1.0  
16 standard deviations (top dashed blue line). This resulted in 2005, 2007, 2010 and 2012 being  
17 classified as ED-AF years and excluded from any trend analysis. We experimented with the  
18 size/shape of the domain to test whether 2015 should also be included as an ED-AF year, but at no  
19 point did either products' standardised anomaly reach 1.0 standard deviation.

20

21 *Artificial Background NO<sub>x</sub> Trends*

22 TCNO<sub>2</sub> from OMI has been subject to the OMI row anomaly (reduced quality of the radiance data at  
23 all wavelengths for a particular viewing angle; KNMI, 2012) for the latter years of the data record.

24 This row anomaly, though partially filtered out using the product quality flags (Braak, 2010)  
25 provided, still yields “striping” issues with the data, especially in later years. This is when background  
26 TCNO<sub>2</sub> is artificially increased, which is evident in the biomass burning season (ASO) as seen in **Figure**

27 **SM2a** (2006), **b** (2009) and **c** (2014). Over the Amazon the artefact is more difficult to detect, but  
28 over the Pacific Ocean and north-western South America the data is becoming noisier with time and  
29 clear data “stripes” occur. When a linear least squares trend is calculated in the ASO mean 2005-  
30 2016 TCNO<sub>2</sub> time-series, there are positive ( $0.05\text{--}0.1 \times 10^{15}$  molecules/cm<sup>2</sup>/year, **Figure SM2d**) TCNO<sub>2</sub>  
31 trend regions with no or limited NO<sub>x</sub> (nitrogen oxides, NO+NO<sub>2</sub>) sources (i.e. over the ocean). This  
32 strongly suggests an artificial instrument space and time-dependent issue yielding false positive  
33 background TCNO<sub>2</sub> trends. To remove these artificial trends from the domain, the average  
34 background ASO 2005–2016 TCNO<sub>2</sub> percentage trend was calculated in each of the blue boxes  
35 (**Figure SM2d**) and then spatially interpolated across the entire domain. The top-left box is not  
36 directly in the corner of the domain as source regions exist there. The blue dashed contour lines  
37 represent the estimated size of the artificial background trend. This 2-D background trend field was  
38 then used to de-trend all OMI TCNO<sub>2</sub> time-series (i.e. one time series per grid box) in the domain  
39 yielding more robust trends shown in **Figure 2c** of the main manuscript. Background regions where  
40 the OMI row anomaly introduced excessively large artificial trends (i.e. grid boxes where TCNO<sub>2</sub> is  
41 less than  $1.5 \times 10^{15}$  molecules/cm<sup>2</sup> and has a positive trend greater than 5%) were removed from  
42 the analysis.

43

#### 44 **SM 2: TOMCAT Ozone (O<sub>3</sub>) Evaluation**

##### 45 ***Surface Observations***

46 Surface observations of O<sub>3</sub> (blue) are from Manaus (60.2°W, 2.6°S) in the Amazon and compared  
47 with the TOMCAT model (red) in **Figure SM3**. This site is representative of background Amazon  
48 conditions with data between 2010 and 2011 covering all months (**Figure SM3**). There is a clearly  
49 defined O<sub>3</sub> seasonal cycle with minimum (4-6 ppbv) concentrations from January to May and peak  
50 (13-15 ppbv) concentrations in August/September. The model reproduces this seasonal cycle, but is  
51 less well defined as it overestimates the observations by 7-8 ppbv between January and May.  
52 However, there is overlap between the model and observational variability (standard deviations). In

53 the biomass burning season (ASO) the model is in good agreement peaking at 15 ppbv. From June-  
54 December, the model seasonal cycle sits within the observational variability and successfully  
55 reproduces the Manaus O<sub>3</sub> concentrations.

56

57 **SAMBBA Aircraft Observations and Ozonesondes**

58 NO<sub>2</sub> and O<sub>3</sub> aircraft (out of plume) data from The South American Biomass Burning Analysis  
59 (SAMBBA; Darbyshire et al., 2019) campaign (September-October, 2012) have been averaged  
60 spatially to produce regional vertical profiles (**Figure SM4**). Here model output was co-located in  
61 time and space to the aircraft observations before both data sets were averaged into vertical  
62 profiles. In the lower troposphere, the model successfully reproduces the seasonal-regional aircraft  
63 O<sub>3</sub> profile (left panel) ranging from 30 ppbv near the surface to 50 ppbv at 2 km. At 2-3 km and  
64 above 4 km, TOMCAT underestimates (~10-15 ppbv) the SAMBBA O<sub>3</sub> profile. The model  
65 underestimation above 4 km is consistent with comparisons to ozonesondes at Natal for 2008  
66 (**Figure SM5**). The nearest ozonesonde data, provided by the SHADOZ project, to the Amazon is from  
67 the Natal site and only available for 2007-2008. The model also underestimates O<sub>3</sub> (by 15-20 ppbv)  
68 at 600-400 hPa (approximately 4-6 km). The model chemical tropopause (i.e. altitude at which O<sub>3</sub> =  
69 100 ppbv) is too low in the model (around 250 hPa) where the model overestimates the  
70 observations by 30-35 ppbv. However, in the boundary layer, the model and ozonesonde profiles  
71 have reasonable agreement.

72

73 For a global model, TOMCAT performs reasonably well in capturing the observed NO<sub>2</sub> vertical profile.  
74 Global models typically struggle to reproduce NO<sub>2</sub> observations given the short NO<sub>x</sub> lifetime and  
75 their coarse horizontal/vertical resolutions (Monks et al., 2017). Near the surface, the model  
76 underestimates by 0.05-0.07 ppbv but this is within the observational variability. In the lower  
77 troposphere (1-3 km), the model successfully captures the observational profile shape, but the  
78 model low bias (0.05 ppbv) is outside the observational variability range.

79

80 Overall, the TOMCAT model successfully captures the Amazon O<sub>3</sub> seasonality and absolute  
81 concentrations in the lower troposphere. This provides us with sufficient confidence in the model's  
82 O<sub>3</sub> simulations used in the main manuscript to investigate long-term changes in surface O<sub>3</sub> and the  
83 corresponding health impacts.

84

### 85 **SM 3: TOMCAT O<sub>3</sub> Seasonality and Trends**

#### 86 ***Seasonality***

87 Peak model-simulated surface O<sub>3</sub> occurs in ASO and reaches over 50 ppbv in the central Amazon  
88 (**Figure SM6**) during the biomass burning season. Minimum concentrations are in December-April  
89 over north-western South America. Throughout the year, O<sub>3</sub> production is simulated from the large  
90 Brazilian cities (e.g. Rio de Janeiro) ranging from ~30 ppbv in May to ~40 ppbv in September.  
91 Between November-April, there is clear outflow of O<sub>3</sub> from the central African fires entering the top-  
92 right of the domain (30-40 ppbv). However, between July and October, O<sub>3</sub> produced from southern  
93 African fire activity dominates concentrations over the South Atlantic (25-35 ppbv).

94

95 When South American fire emissions are switched off (TOMCAT "fire-off" simulation, **Figure SM7**)  
96 there is a small decrease in surface O<sub>3</sub> (several ppbv) between November-June. However, in July-  
97 October there is a large drop in O<sub>3</sub> concentrations over the Amazon with peak reductions (20-30  
98 ppbv) in September. As no fire precursor gases are emitted there is no excess O<sub>3</sub> formation during  
99 the ASO season. In **Figure SM8**, Eastern Brazil (red) and Wider Amazon Region (blue) (see boxed area  
100 in **Figure 4d** of the main manuscript) seasonal cycles show enhanced domain-average surface O<sub>3</sub> (20-  
101 30 ppbv) in July-October (top panel). When fire emissions are switched off (middle panel), there is  
102 no seasonality with concentrations of 15-16 ppbv. The fire emission contributions to average surface  
103 O<sub>3</sub> (bottom) is approximately 0-1 ppbv from January to June in both domains. However, in August

104 and September, fire emission contributions jump to 10-11 ppbv in the Amazon Region. Over Eastern  
105 Brazil, the peak O<sub>3</sub> contributions are 12-14 ppbv in ASO.

106

107 **Surface Trends**

108 **Figure 4a & b** of the main manuscript show significant (90% confidence level; 90%CL) trends in  
109 TOMCAT model ASO average surface NO<sub>2</sub> and O<sub>3</sub> concentrations between 2005 and 2016. To  
110 investigate whether pollutant trends were qualitatively similar to OMI TCNO<sub>2</sub> trends (**Figure 2c** of  
111 the main manuscript), average regional trends (black box region in **Figure 2a** of the main manuscript)  
112 were calculated over the Cerrado Region. Here, significant (90%CL) positive trends (**Figure SM9**) are  
113 found when the ED-AF years (2005, 2007, 2010 and 2012 – hollow circles) are removed from the  
114 analysis, supporting the satellite observed trends.

115

116 **References:**

117 Aragão, L. E. O. C., Poulter, B., Barlow, J. B., Anderson, L. O., Malhi, Y., Saatchi, S., et al. (2014).  
118 Environmental change and the carbon balance of Amazonian forests. *Biological Reviews* **89**, 913-931.  
119 <https://doi.org/10.1111/brv.12088>.

120

121 Braak, R. Row Anomaly Flagging Rules Lookup Table, *KNMI Technical Document TN-OMIE-KNMI-*  
122 *950*, 2010.

123

124 Darbyshire, E., Morgan, W. T., Allan, J. D., Liu, D., Flynn, M. J., Dorsey, J. R., et al. (2019). The vertical  
125 distribution of biomass burning pollution over tropical South America from aircraft in situ  
126 measurements during SAMBBA. *Atmospheric Chemistry and Physics* **19**, 5771-5790.

127 <https://doi.org/10.5194/acp-19-5771-2019>.

128

129 Monks, S. A., Arnold, S. R., Hollaway, M. J., Pope, R. J., Wilson, C., Feng, W., et al. (2017). The  
130 TOMCAT global chemistry transport model v1.6: description of chemical mechanism and model  
131 evaluation. *Geophysical Model Development* **10**, 3025-3057. [https://doi.org/10.5194/gmd-10-3025-  
132 2017.](https://doi.org/10.5194/gmd-10-3025-2017)

133

134 Reddington, C. L., Butt, E. W., Ridley, D. A., Artaxo, P., Morgan, W. T., Coe, H. & Spracklen, D. V.  
135 (2015). Air quality and human health improvements from reductions in deforestation-related fires in  
136 Brazil, *Nature Geoscience* **8**, 768-773. <https://doi.org/10.1038/ngeo2535>.

137

138 Royal Netherlands Meteorological Institute (KNMI). Background information about the Row Anomaly  
139 in OMI (2012). Available: [http://projects.knmi.nl/omi/research/product/rowanomaly-  
140 background.php](http://projects.knmi.nl/omi/research/product/rowanomaly-background.php) (last accessed 26/09/2018).

141

142

143

144

145

146

147

148

149

150

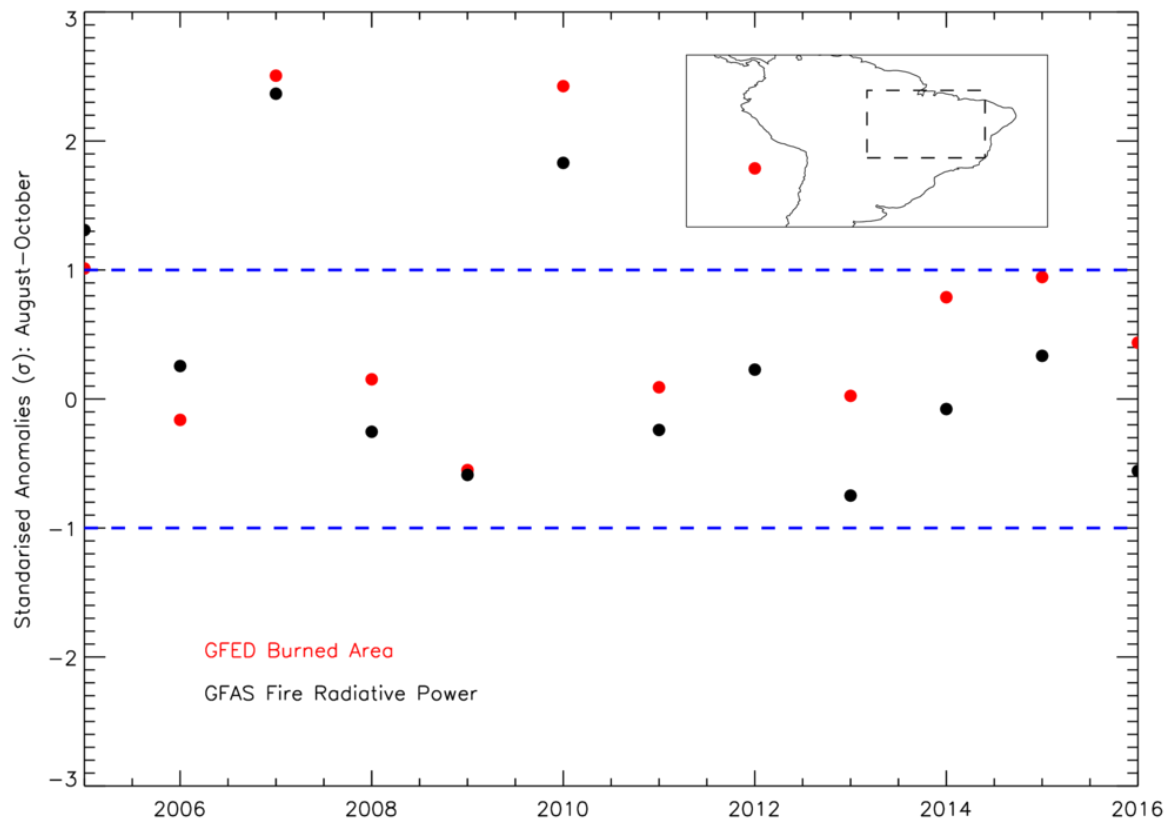
151

152

153

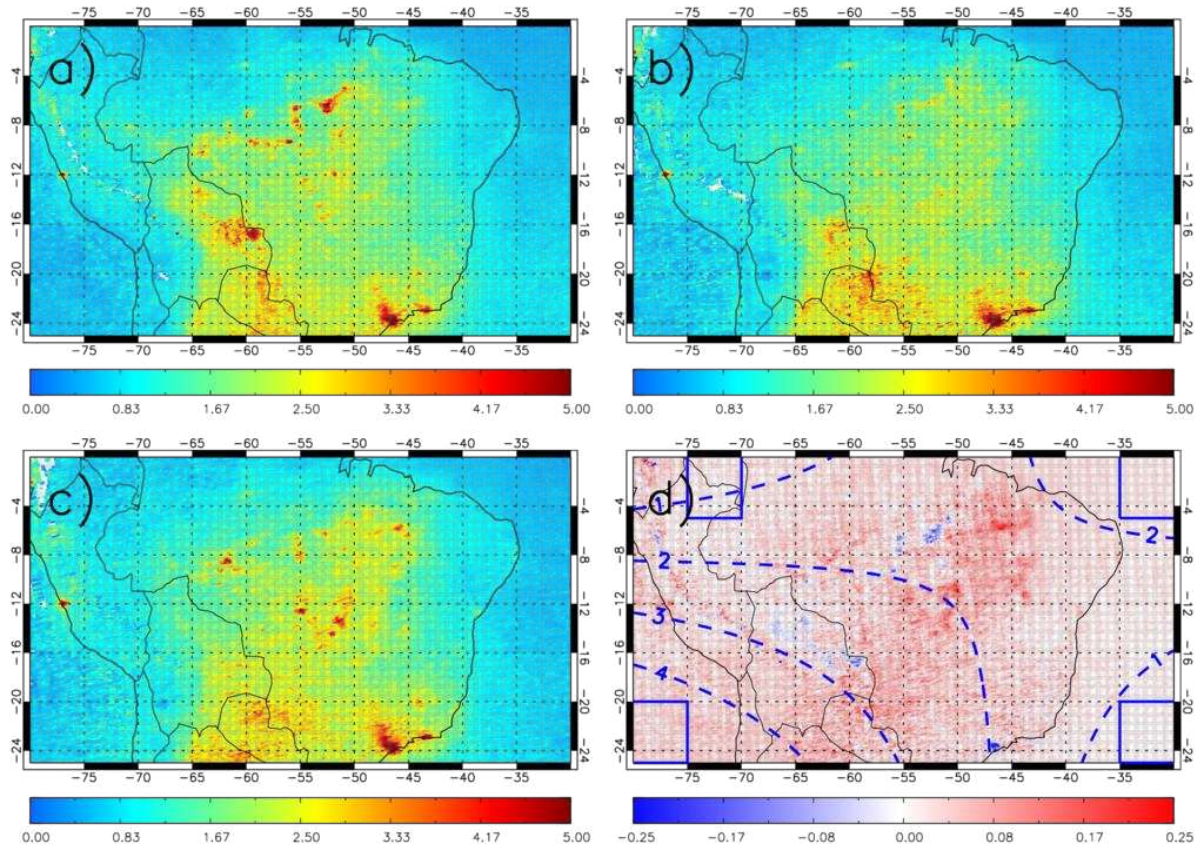
154

155    **Supplementary Figures:**



156

157    **Figure SM1:** Annual average standardised anomalies for GFED Fire-Burned-Area (FBA, red) and GFAS  
158    Fire Radiative Power (FRP, black) calculated over North-Eastern South America (black dashed  
159    region). Blue dashed lines show the  $\pm 1.0$  standard deviations.

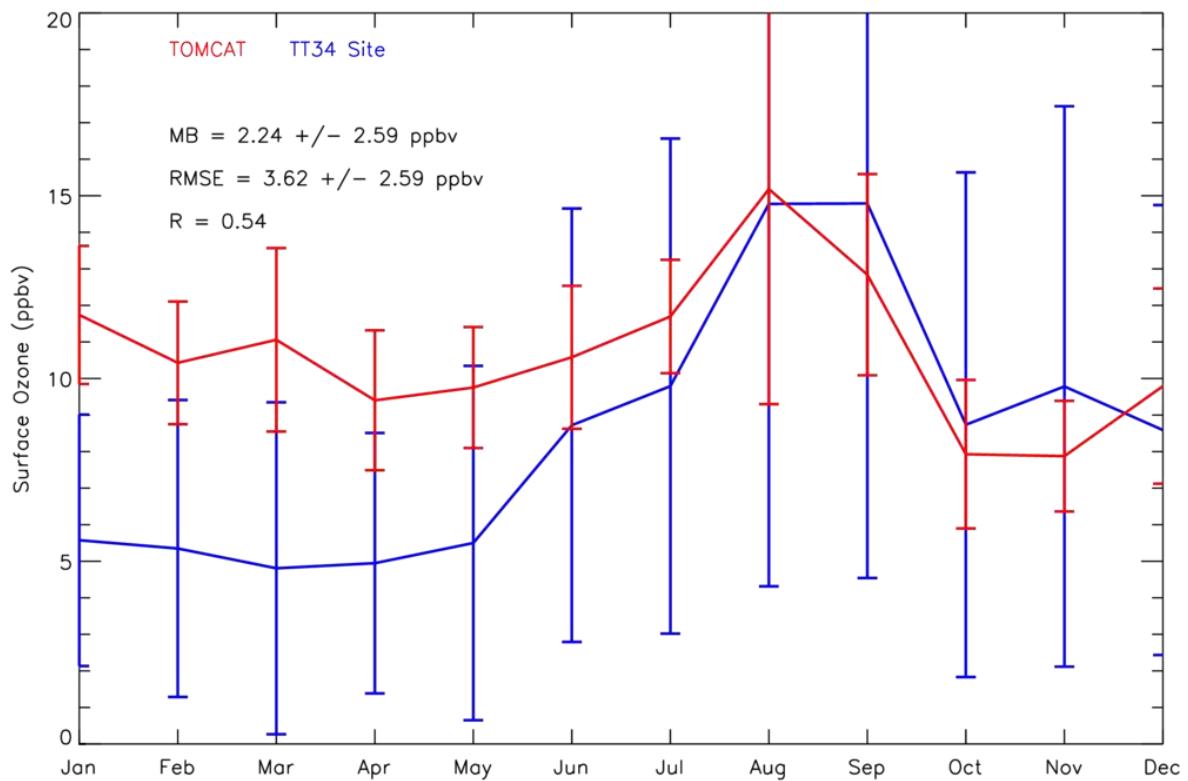


160

161 **Figure SM2:** Demonstration of deterioration of OMI TCNO<sub>2</sub> ( $10^{15}$  molecules/cm<sup>2</sup>) retrieved over  
162 background regions (e.g. the ocean) for the ASO average in a) 2006, b) 2009 and c) 2014. The ASO  
163 trend ( $10^{15}$  molecules/cm<sup>2</sup>/year) between 2005 and 2016 is shown in panel d). The blue boxes  
164 highlight the regions used to calculate the positive artificial background trends (%) mapped over the  
165 domain, used to de-trend the OMI TCNO<sub>2</sub> record.

166

167



168

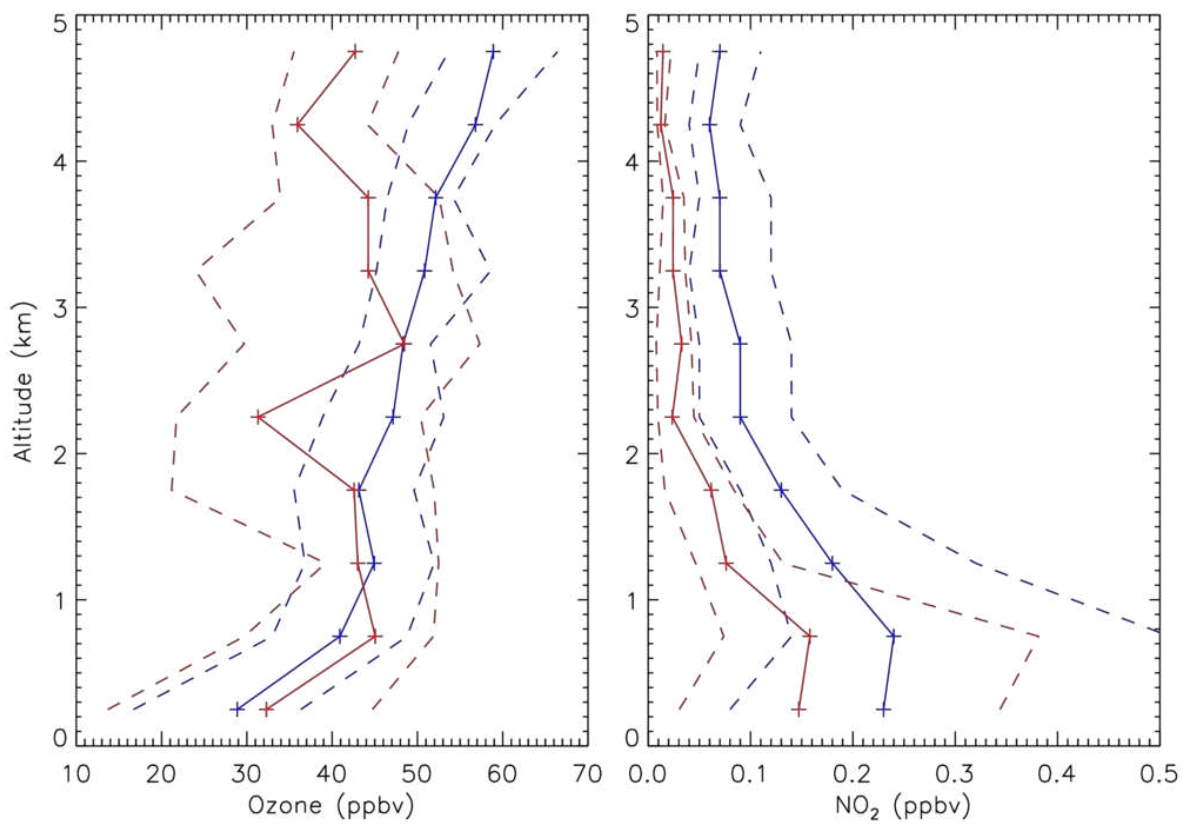
169 **Figure SM3:** Average surface O<sub>3</sub> (ppbv) seasonal cycle for 2010-2011 at Manaus (TT34), Brazil

170 (60.2°W, 2.6°S). Observations and model seasonal cycles are shown in blue and red, respectively.

171 Observational and model variability is represented by the monthly standard deviations.

172

173



174

175 **Figure SM4:** Median aircraft (blue) and modelled (red) profiles from the SAMBBA campaign

176 (September-October, 2012) of O<sub>3</sub> (left panel, ppbv) and NO<sub>2</sub> (right panel, ppbv) over the Amazon.

177 Dashed lines represent the 25<sup>th</sup> and 75<sup>th</sup> percentiles in the model and aircraft data.

178

179

180

181

182

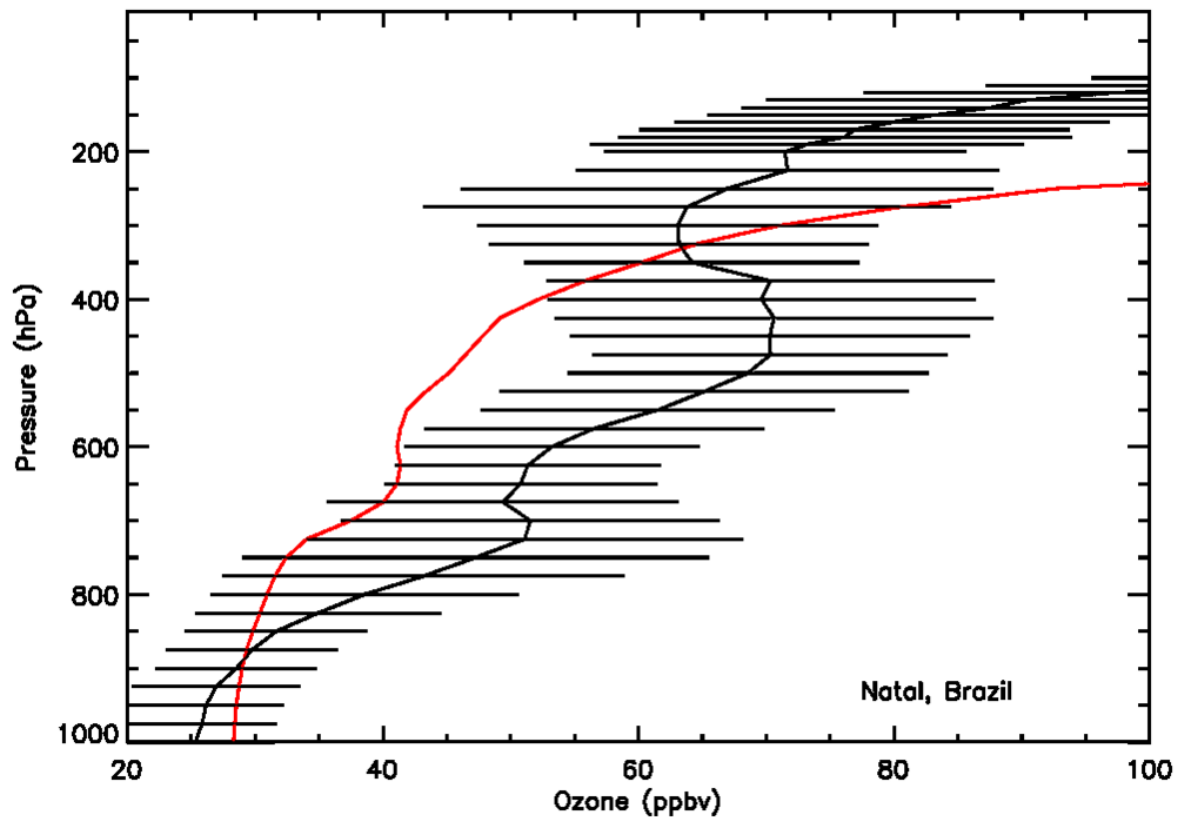
183

184

185

186

187



188

189 **Figure SM5:** Averaged ozonesonde (black) and model (red) vertical O<sub>3</sub> profiles (ppbv) for July-  
190 November (2007-2008) at Natal, Brazil. Black horizontal lines represent the observational variability  
191 (standard deviation).

192

193

194

195

196

197

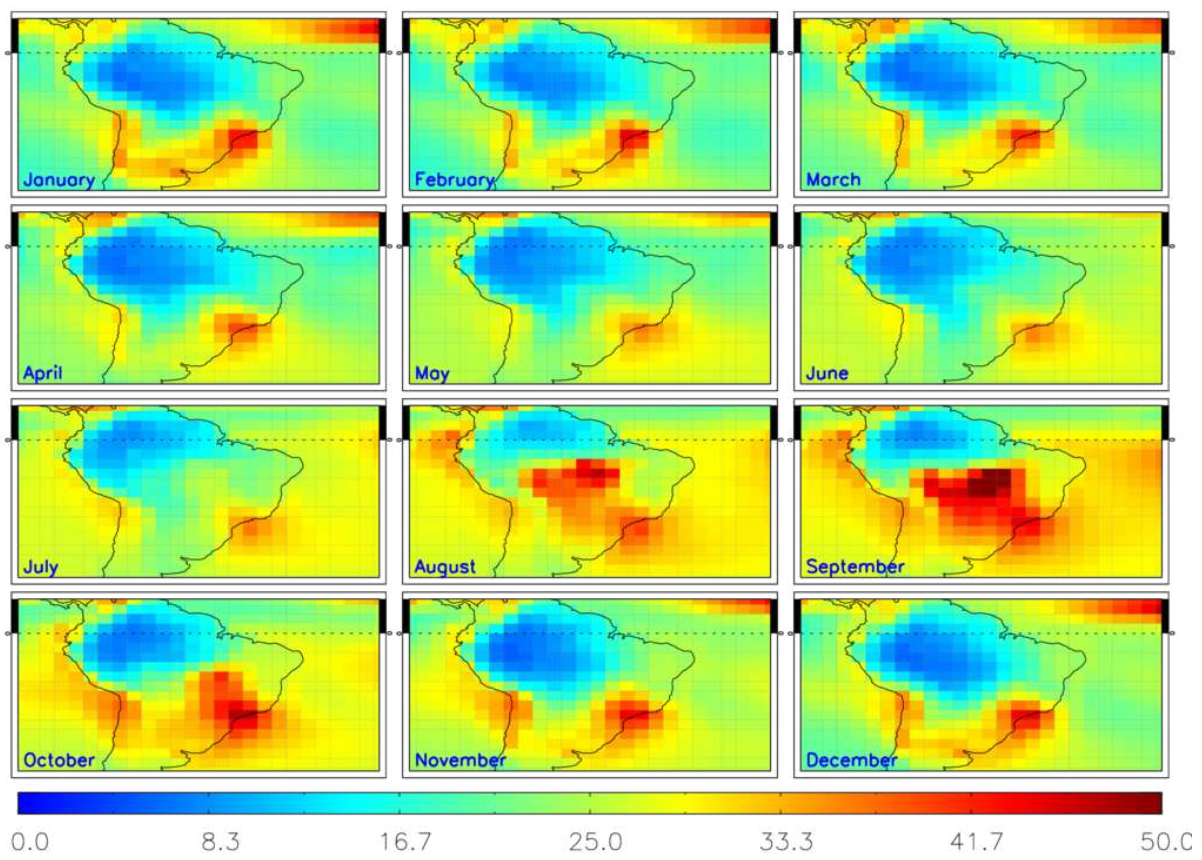
198

199

200

201

202



203      0.0      8.3      16.7      25.0      33.3      41.7      50.0

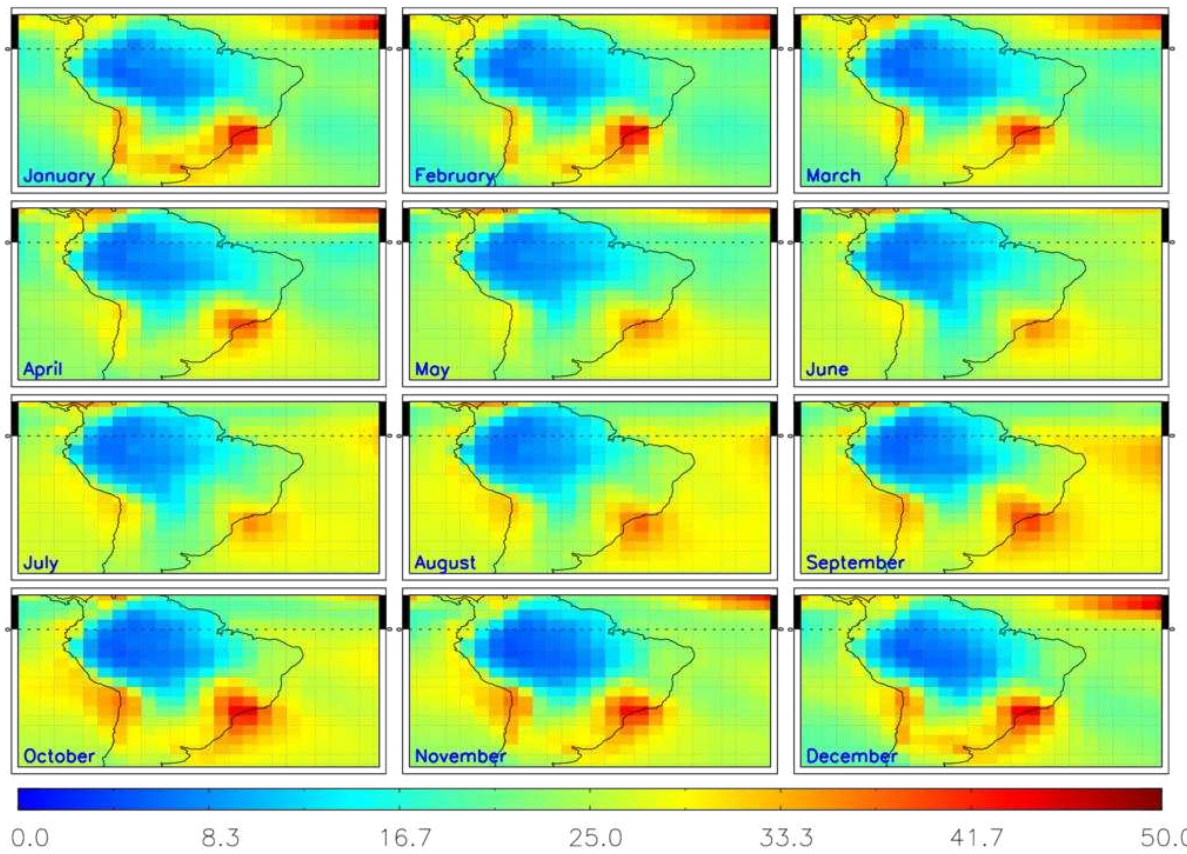
204 **Figure SM6:** Mean TOMCAT surface O<sub>3</sub> (ppbv) seasonal cycle (2005-2016 average) over South  
205 America from the simulation which includes fire emissions (fire-ctl).

206

207

208

209



210            0.0            8.3            16.7            25.0            33.3            41.7            50.0

211 **Figure SM7:** Mean TOMCAT surface O<sub>3</sub> (ppbv) seasonal cycle (2005-2016 average) over South  
212 America from the simulation without fire emissions (fire-off).

213

214

215

216

217

218

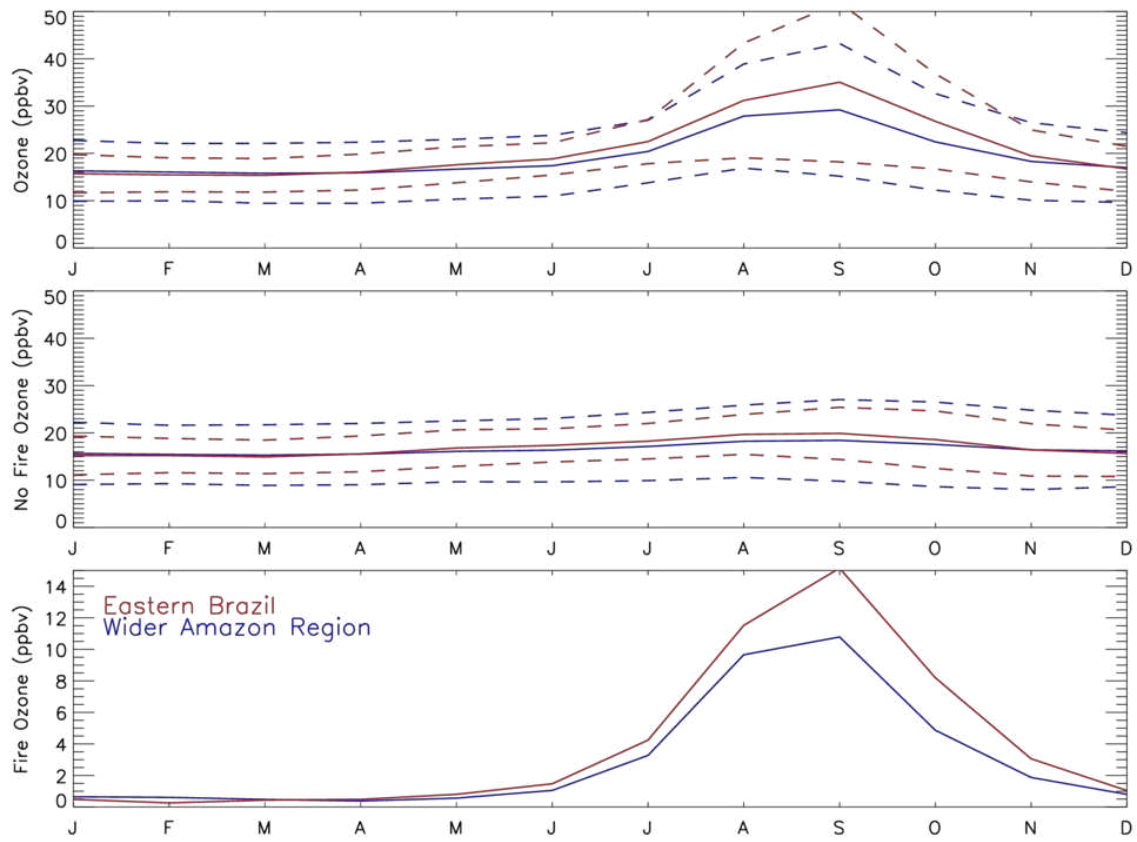
219

220

221

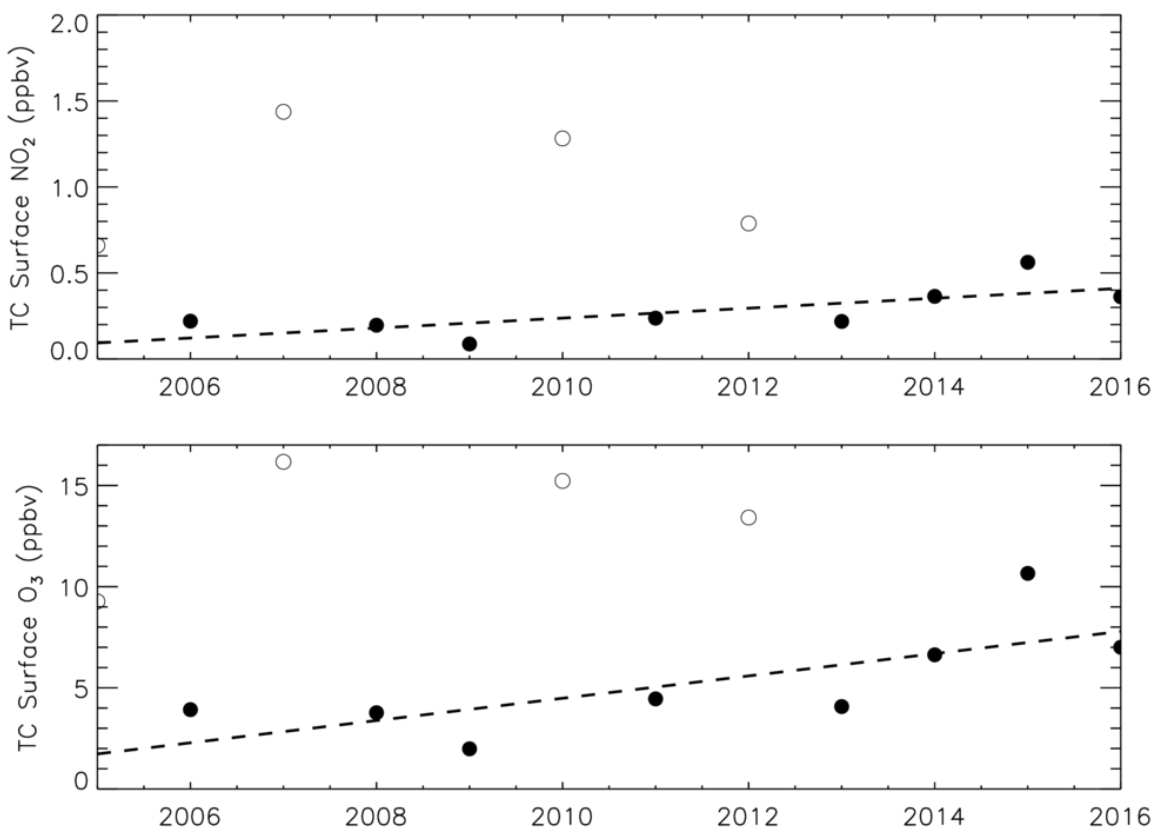
222

223



224

225 **Figure SM8:** TOMCAT surface  $O_3$  (ppbv) seasonal cycle (2005-2016 average) for the Wider Amazon  
 226 Region (blue) and Eastern Brazil (red; see **Figure 4** of the main manuscript). Surface  $O_3$  from the  
 227 TOMCAT “fire-ctl” simulation, “fire-off” simulation and “fire-ctl” - “fire-off” difference are shown in  
 228 the top, middle and bottom panels, respectively. Dashed lines represent the monthly standard  
 229 deviations.



230

231 **Figure SM9:** TOMCAT surface NO<sub>2</sub> (ppbv, top panel) and O<sub>3</sub> (ppbv, bottom panel) averaged over the  
 232 black box in Figure 2a (main manuscript) for August-September-October (ASO) between 2005 and  
 233 2016. Hollow circles represent extreme drought –anomalous fire (ED-AF) years. Black dashed lines  
 234 show significant trends (90%CL).

235

236

237

238

239

240

241

242

243